Liquid Crystals
Publication details, including instructions for authors and subscription information:
http://www.informaworld.com/smpp/title~content=t713926090

Structural characterization of the smectic polymorphism of chiral liquid crystalline polysiloxanes containing biphenyl mesogens

Bernard Gallot[a]; Giancarlo Galli[b]; Eleftheria Dossi[b]; Emo Chiellini[b]
[a] Laboratoire des Matériaux Organiques à Propriétés Spécifiques, CNRS, Vernaison, France [b] Dipartimento di Chimica e Chimica Industriale, Università di Pisa, Pisa, ITALY

To cite this Article Gallot, Bernard , Galli, Giancarlo , Dossi, Eleftheria and Chiellini, Emo(1995) 'Structural characterization of the smectic polymorphism of chiral liquid crystalline polysiloxanes containing biphenyl mesogens', Liquid Crystals, 18: 3, 463 — 473
To link to this Article: DOI: 10.1080/02678299508036646
URL: http://dx.doi.org/10.1080/02678299508036646

LIQUID CRYSTALS, 1995, VOL. 18, NO. 3, 463–473

Structural characterization of the smectic polymorphism of chiral liquid crystalline polysiloxanes containing biphenyl mesogens

by BERNARD GALLOT

Laboratoire des Matériaux Organiques à Propriétés Spécifiques, CNRS, BP 24, 69390 Vernaison, France

GIANCARLO GALLI, ELEFTHERIA DOSSI and EMO CHIELLINI*

Dipartimento di Chimica e Chimica Industriale, Università di Pisa, Via Risorgimento 35, 56126 Pisa, Italy

(*Received 18 February 1994; in final form 10 June 1994; accepted 24 June 1994*)

A structural characterization of chiral side chain siloxanes with different average degrees of polymerization, DP_n, was performed by X-ray diffraction experiments on powder and oriented fibre specimens. Polymers ($DP_n = 35$) and oligomers ($DP_n = 4$) contained the 4,4′-biphenylene unit with either an (*S*)-2-methylbutoxy (**An**, **Bn**) or an (*S*)-2-chloro-3-methylbutanoyloxy substituent (**C11**). The spacer segment connected to the siloxane backbone had a variable number, *n*, of methylene groups ($n = 5$, 8, or 11). Independent of the spacer length and the chiral tail nature, the polysiloxanes underwent the same sequence of phases: C–S_{F_i} (or S_{I_i})–S_{C_i}–S_{A_1}–I, whereas in the oligosiloxanes the sequence C–S_{B_1}–S_{A_1}–I (**B11**) or C–S_{F_i}–S_{C_i}–I (**B5**) occurred. The influence of the structure of the polysiloxanes on the formation of the smectic (tilted or orthogonal) mesophases was elucidated. The rather large number of reflections (three or four) detected in the X-ray patterns at low angles, allowed a drawing of the projection of the electron density profiles along the layer normal, $\rho(z)$, and deduction of the most physically acceptable electron density profiles from among the numerous possibilities for each smectic phase. The electron density profiles were in agreement with monolayer smectic phases presenting a microphase separation between the siloxane backbones and the side chains, so constraining the polymer backbones within a thin layer.

1. Introduction

Ferroelectric liquid crystals are the focus of intense research activity, especially for devising high information content displays [1]. After the first prediction and discovery of ferroelectricity in chiral smectic C liquid crystals [2], a variety of new phases with associated relevant electro-optical effects has been described, and currently the term ferroelectric liquid crystal may be understood in a broader sense to include also antiferroelectric, ferrielectric, and electroclinic materials [3].

Chiral liquid crystalline polymers can present various electro-optical effects [4] in their chiral mesophases by analogy with low molar mass counterparts. However, incorporation of mesogenic units and chiral group substituents into a polymer structure results in rather peculiar structures and properties of the liquid crystalline polymers. In particular, fixation of chiral mesogens at one end to a polymer backbone generally leads to a rich liquid crystal polymorphism of side chain polymers [5], which is in contrast to that most typical of small molecule liquid crystals with a strong longitudinal dipole.

* Author for correspondence.

Very recent investigations have evidenced the formation of additional unconventional structures in chiral liquid crystalline polymers [6] that in turn might be related to the existence of unusual electro-optical responses of smectic mesophases [7], including the availability of multiple switching states [8–10]. Therefore, the structural characterization of liquid crystalline polymers can help to address the question of their eventual use in electro-optics.

Within this scope, we are studying chiral side chain polymers of different chemical and stereochemical structures [11–13] in order to assess the potential application of tilted (ferroelectric) and orthogonal (electroclinic) smectic polymers in electro-optical devices [14, 15]. In this paper we report on the structural characterization of chiral side chain siloxanes with different average degrees of polymerization (DP_n). Polysiloxanes ($DP_n = 35$) and oligosiloxanes ($DP_n = 4$) contained the 4,4′-biphenylene mesogenic group bearing either the (*S*)-2-methylbutoxy (**An**, **Bn**) or the (*S*)-2-chloro-3-methylbutanoyloxy substituent (**C11**). The mesogenic unit was connected to the siloxane backbone by a spacer segment with a variable number *n* of methylene groups ($n = 5$, 8, or 11).

0267–8292/95 $10·00

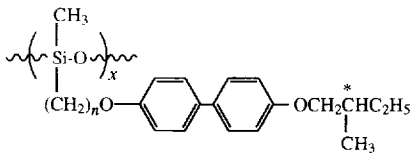

An $x=35$ ($n=5$, 8, 11) **An, Bn**
Bn $x=4$ ($n=5$, 11)

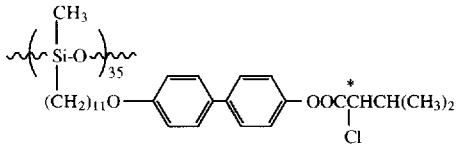

C11

These samples were expected to present a rich smectic polymorphism, and their ferroelectric and electroclinic properties are presently being investigated. X-ray diffraction measurements were performed on both powder and fibre samples, and from the intensity of the diffraction signals in the low-angle region the electron density profiles along the smectic layer normal were estimated, and the most physically acceptable ones were identified.

2. Experimental

2.1. *Synthesis of materials*

Side chain monomers were synthesized according to general procedures previously described [12, 16]; polysiloxanes ($DP_n=35$) and oligosiloxanes ($DP_n=4$) were prepared by grafting the monomers onto the corresponding commercially available (from Petrarch) poly- and oligo-(hydrosiloxane)s [11]. The synthesis of **B11** is reported here as a typical example of this class of materials.

Oligo{methyl 11-[4'-((S)-2-methylbutoxy)-4-biphenylene]undecyloxy}siloxane (**B11**)

0·132 g (2·2 mmol of Si–H group) of oligo(methylhydrosiloxane) ($DP_n=4$), 1 g (2·5 mmol) of 4-(10-undecenyloxy)-4'-((*S*)-2-methylbutoxy)biphenyl were dissolved in 30 ml of anhydrous toluene under nitrogen. 0·03 ml (0·005 mmol) of a 3·3 per cent solution of platinum divinyltetramethyldisiloxane in xylene was then added with a microsyringe and the solution was heated to 50°C for 18 h. After cooling down to room temperature, the reaction mixture was poured into 200 ml of methanol and the precipitated polymer was filtered off and purified by repeated precipitations from chloroform solution into methanol and extraction with diethyl ether: yield 68 per cent; $[\alpha]_D^{25}+6·0°$ ($CHCl_3$, $c=2·5\,g\,dl^{-1}$). ^1H NMR ($CDCl_3$) δ_H 7·3 (s, 4 H), 6·8 (s, 4 H), 3·8 (m, 4 H), 1·8 (s, 3 H), 1·6 (s, 3 H), 1·2 (m, 1 H), 0·9 (m, 6 H), 0·6 (s, 2 H), 0·1 (m, 7·5 H) in ppm.

2.2. *Characterization*

X-ray diffraction experiments were performed on powder samples with a Guinier-type focusing camera operating under vacuum, equipped with a bent quartz monochromator (reflection 101) giving a linear collimation of strictly monochromatic X-rays ($CuK_{\alpha 1}$, $\lambda=1·54$ Å) and a device for recording the diffraction patterns at various temperatures between 20 and 200°C with an accuracy of ± 1°C. Several exposures were made so as to measure the strongest and the weakest reflections. Experimental amplitudes, a_m, of diffraction of the different orders of reflections from the smectic layers were corrected for the Lorentz-polarization factor [17] and normalized to the amplitude of the respective first order (see table 1). As exposure times with the focusing camera were rather long, a home-made pinhole camera, operating under vacuum, using Ni-filtered Cu radiation was also used. This camera was equipped with an electric heating device operating between 20 and 300°C with an accuracy of ± 1°C, and especially designed to operate with capillaries containing powder or fibre samples.

3. Results and discussion

Liquid crystalline polysiloxanes **An** and **C11** and oligosiloxanes **Bn** were prepared by grafting the corresponding side chain alkene monomers onto preformed hydrosiloxanes of different molecular weights ($DP_n=35$ or 4) in the presence of a platinum catalyst, according to [11]. Between the glass transition temperature (T_g) and the isotropization temperature (T_i), four phases were detected for each polysiloxane, while three phases were observed for each oligosiloxane. The smectic phases occurred in various sequences. No evidence was obtained of the existence of a nematic phase. The phase transitions, with relevant thermodynamic parameters, for the polymers and the oligomers are summarized in tables 2 and 3, respectively.

In general, X-ray diagrams of the different phases exhibited, in the low-angle region, a set of one to four reflections with Bragg spacings in the ratio 1:2:3:4 characteristic of a layered structure, but they differed by the aspect of their wide-angle domains (see figure 1 (*a*)–(*c*)). For the phases covering the temperature range

Table 1. Amplitude† and electron density values for polysiloxanes and oligosiloxanes.

Sample	Mesophase	a_1	a_2	a_3	a_4	ρ_0/e Å^{-1}
A5	S_{A_1}	1	0·5	0·08	0	8·4
A8	S_{F_1}	1	0·5	0·2	0	8·1
A11	S_{A_1}	1	0·5	0·3	0	7·7
B5	S_{C_1}	1	0·5	0·1	0	8·4
B11	S_{A_1}	1	0·5	0·25	0	7·8
	S_{B_1}	1	0·4	0·05	0	7·8
C11	S_{A_1}	1	0·5	0·35	0·3	8·3

† After normalization to the amplitude value of the first order reflection.

Table 2. Phase transition parameters† of polysiloxanes‡ **An** and **C11**.

Sample	n	T_g/K	T_m/K	ΔH_m/kJ mol^{-1}	$T_{S_1-S_2}$/K	$\Delta H_{S_1-S_2}$/kJ mol^{-1}	$T_{S_2-S_3}$/K	$\Delta H_{S_2-S_3}$/kJ mol^{-1}	T_I/K	ΔH_I/kJ mol^{-1}
A5	5	321	404	3·9	407	n.d.§	412	1·3	429	7·4
A8	8	319	399	3·4	405	4·0	414	0·9	428	6·0
A11	11	319	370	1·3	387	2·5	397	0·7	429	7·5
C11	11	311	359	2·5	373	n.d.§	381	n.d.§	439	5·7

† Glass transition temperature (T_g), and melting (m), smectic–smectic (S_1–S_2, S_2–S_3), and isotropization (I) phase transition temperatures and enthalpies (see text).
‡ Average degree of polymerization = 35.
§nd = not detected by DSC.

between room temperature and the melting temperature (T_m), the wide-angle region showed three sharp reflections characteristic of a crystalline (or highly ordered smectic phase) (see figure 1 (*a*)). Above this temperature, in all cases the wide-angle domain exhibited only one rather sharp reflection typical of an ordered smectic phase with hexagonal packing of the side chains (see figure 1 (*b*)), which then turned into the diffuse band of a disordered smectic (see figure 1 (*c*)) at a transition temperature $T_{S_1-S_2}$ as given in tables 2 and 3. This pattern remained practically unchanged up to the isotropization temperature for the oligomers, whereas the polymers underwent an additional transition at a temperature noted as $T_{S_2-S_3}$ in table 2. We will describe first the behaviour of the polysiloxanes and then that of the oligosiloxanes.

3.1. *Structure of the polysiloxanes* **An** *and* **C11**

Polymer samples **A11**, **A8**, and **A5**, exhibited three wide-angle reflections below their respective melting tem-

Table 3. Phase transition parameters† of oligosiloxanes‡ **Bn**.

Sample	n	T_g/K	T_m/K	ΔH_m/kJ mol^{-1}	$T_{S_1-S_2}$/K	$\Delta H_{S_1-S_2}$/kJ mol^{-1}	T_I/K	ΔH_I/kJ mol^{-1}
B5	5	315	388	8·9	395	n.d.§	411	12·1
B11	11	313	373	1·0	390	1·1	410	11·0

† Glass transition temperature (T_g), and melting (m), smectic–smectic (S_1–S_2), and isotropization (I) phase transition temperatures and enthalpies (see text).
‡ Average degree of polymerization = 4.
§nd = not detected by DSC.

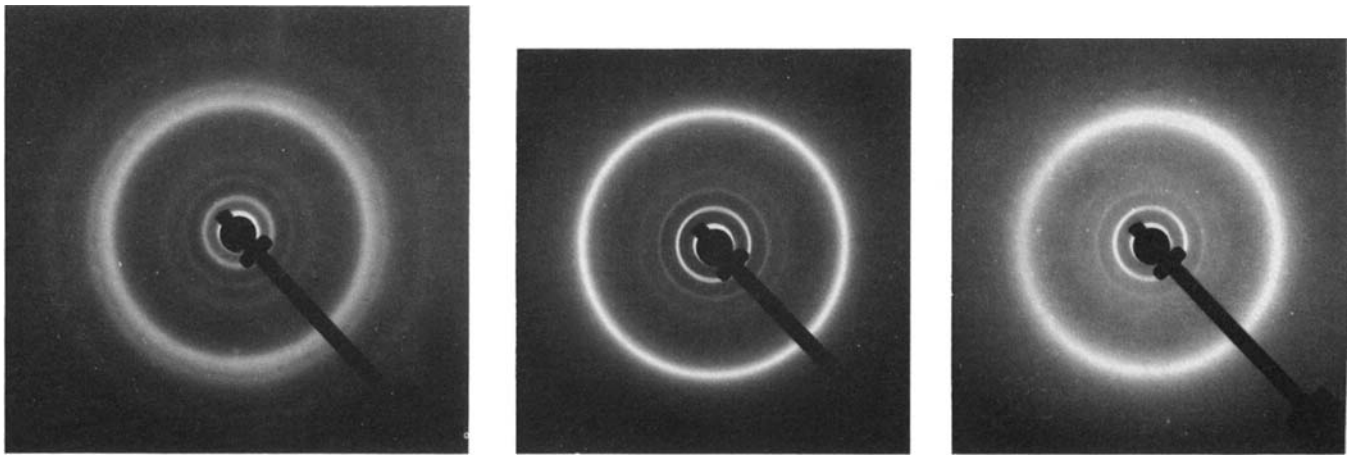

(*a*) (*b*) (*c*)

Figure 1. X-ray powder diagrams of polysiloxane **A11** obtained with the pinhole camera (*a*) triclinic at room temperature, (*b*) S_{F_1} at 110°C, and (*c*) S_{A_1} at 130°C.

peratures. As we do not know the symmetry space group, they might tentatively be indexed as the (1,0), (0,1), and (1,1) reflections of an oblique lattice with parameters $a=4{\cdot}4$ Å, $b=4{\cdot}0$ Å, and $\beta=85°$. Comparison of the thickness, d, of the lamellae with the length, L (33·0 Å for **A11**, 29·0 Å for **A8**, and 25·5 Å for **A5**), of the fully extended repeating unit of the polymer measured using CPK models gives values of the tilt angle, θ, of 14, 17, and 23°, respectively. The tilted character of these structures was also demonstrated by fibre diagrams (see figure 2). In agreement with the above results, θ values of 15, 18, and 23° were obtained from the fibre patterns. Therefore, this low temperature phase was a three-dimensionally ordered one of triclinic type. The X-ray diagrams of **C11** were very poor and corresponded to a crystalline structure with a low degree of crystallinity.

Above T_m, the X-ray patterns of the polysiloxanes exhibited, in the wide-angle region, one single and rather sharp reflection. In each case, d was slightly shorter than L (see table 4). In low molar mass liquid crystals, the spacing d for various orthogonal smectic phases, like the A, B, or E phases, can be shorter than the calculated molecular length L, due to the conformational freedom of the molecules in the mesophase and their thermal displacement along the director [18, 19]. However, in liquid crystalline polymers, in which the mesogenic side chains are connected to the polymer backbone by means of a spacer segment, their overall motion is more restricted with respect to the rather freely moving molecules of the low molar mass counterparts. In the present

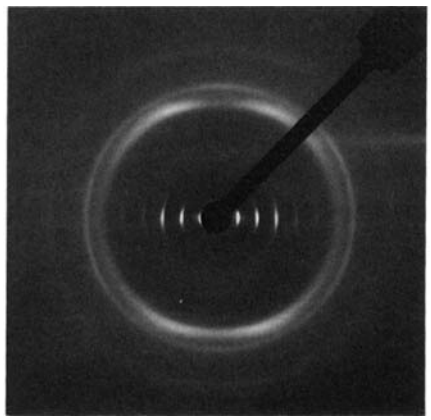

Figure 2. X-ray fibre diagram of the triclinic structure at room temperature of polysiloxane **A11**.

polysiloxanes, incompatibility between the macromolecular chain and the side chains (see below) can impose additional constraints on their mobility, thus reducing their thermal displacement along the director of the smectic phase. Therefore, the above difference between d and L may be accounted for by a tilt of the side chains with respect to the layer normal, such as in a monolayer smectic of the F or I type. The occurrence of tilted mesophases is also consistent with our polarizing microscopy observations (see figure 3). It is difficult to distinguish the S_{F_1} phase (tilt direction towards an edge of the hexagon) from the S_{I_1} phase (tilt direction towards an apex of the hexagon) [20]. Nevertheless, the single

Table 4. Structural parameters† of the different phases of the liquid crystalline siloxanes **An**, **Bn**, and **C11**.

	A5	**A8**	**A11**	**B5**	**B11**	**C11**
$L\pm0{\cdot}5$ Å	25·5	29·0	33·0	25·5	33·0	33·0
Structure	Triclinic	Triclinic	Triclinic	Monoclinic (or S_{H_1})	Monoclinic (or S_{E_1})	C
$d\pm0{\cdot}3$ Å	23·5	27·8	32·0	24·6	33·2	
a/Å	4·4	4·4	4·4	4·8	4·5	
b/Å	4·0	4·0	4·0	3·8	3·9	
β/deg	85	85	85	90	90	
θ/deg	23	17	14	15	0	
Structure	S_{F_1} (or S_{I_1})	S_{F_1} (or S_{I_1})	S_{F_1} (or S_{I_1})	S_{F_1} (or S_{I_1})	S_{B_1}	S_{F_1} (or S_{I_1})
$d/\pm0{\cdot}3$ Å	24·1	28·1	32·4	24·6	33·0	32·4
a/Å	5·2	5·2	5·2	5·0	5·1	5·2
θ/deg	19	14	11	15	0	11
Structure	S_{C_1}	S_{C_1}	S_{C_1}	S_{C_1}	S_{A_1}	S_{C_1}
$d/\pm0{\cdot}3$ Å	24·1	28·1	32·4	24·6	32·6	32·4
a/Å	5·2	5·2	5·2	5·0	5·2	5·2
θ/deg	19	14	11	15	0	11
Structure	S_{A_1}	S_{A_1}	S_{A_1}			S_{A_1}
$d/\pm0{\cdot}3$ Å	25·0	28·5	33·2			33·6
a/Å	5·1	5·1	5·2			5·2

† Tentative values for the triclinic structure of **A5**, **A8**, and **A11**.

outer reflection of the I phase is known to be sharper than that of the F phase [20, 21]. The broadness of the wide-angle reflection of our X-ray powder diagrams suggests that the smectic phases is of the S_{F_1} type.

At the transition temperature $T_{S_1-S_2}$ (see table 2), no variation was observed in the low-angle domain and the thickness of the smectic layers and the tilt angle remained unaffected. However, the wide-angle reflection became more diffuse, consistent with the loss of in-layer correlation due to the transition to a S_{C_1} phase.

Within the highest temperature mesophase (above $T_{S_2-S_3}$ of table 2), the wide-angle region of the X-ray patterns exhibited a diffuse band typical of a disordered smectic. Comparison of the smectic layer thickness with the length of the repeating unit (see table 4) showed that $d=L$, as in the S_{A_1} phase for **A11** and **C11**, whereas d was slightly smaller than L for both **A8** and **A5**; this difference is, however, within the limits of the experimental error.

The occurrence of an ordered (S_F) and two disordered (S_C and S_A) smectic phases is in agreement with the observations by polarizing microscopy of the optical textures in the relevant temperature ranges (see figure 3 (*a*)–(*c*)). Typically, the S_A phase displayed focal-conic patterns with fans, which became broken and striated in the lower temperature S_C phase. The ordered phase falling below it was characterized by the appearance of textures with more broken and truncated fans, but no unambiguous identification of this phase was possible simply by optical microscopy [11]. The phase sequence I–S_A–S_C–S_F seems to be rather common in biphenyl-containing liquid crystals, both low molar mass [22] and polymeric [21], and is also encountered in standard materials for miscibility studies [18]. Furthermore, our investigations of the electro-optical responses of the polymers clearly demonstrate the formation of S_C and S_A phases and their phase transition in agreement with the present data. The electroclinic (S_A) and ferroelectric (S_C) properties of the chiral polysiloxanes will be described elsewhere [23].

3.2. *Structure of the oligosiloxanes* **Bn**

For the two oligosiloxanes **B11** and **B5**, the three wide-angle reflections were indexed as the (1,0), (0,1), and (1,1) reflections of a rectangular lattice with parameters $a=4{\cdot}5$ Å and $b=3{\cdot}9$ Å for **B11**, and $a=4{\cdot}4$ Å and $b=3{\cdot}8$ Å for **B5**. For **B11**, d was equal to L, and so the side chains were perpendicular to the lamellae as in a semicrystalline (or E) phase. For **B5**, the comparison of $d=24{\cdot}6$ Å with $L=25{\cdot}5$ Å showed that the side chains were tilted by $\theta\approx 15°$. Therefore, the structure is monoclinic and corresponds to a semicrystalline structure with a rather low degree of crystallinity (or highly ordered H or K phases [24]).

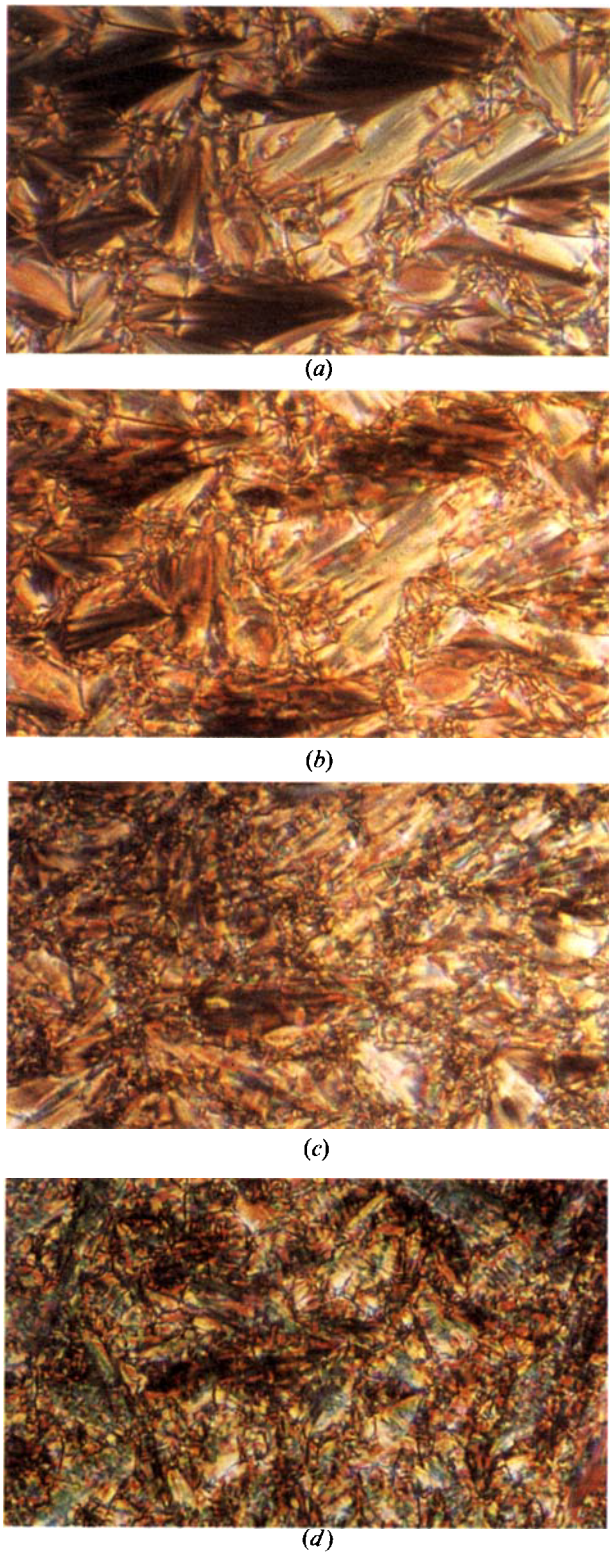

Figure 3. Optical photomicrographs of the textures (on cooling from the isotropic melt) of the mesophases of polysiloxane **A8**: S_{A_1} at 149°C (*a*), S_{C_1} at 136°C (*b*), S_{F_1} (or S_{I_1}) at 128°C (*c*), and oligosiloxane **B5**: at 116°C (*d*) (original magnification 300 ×).

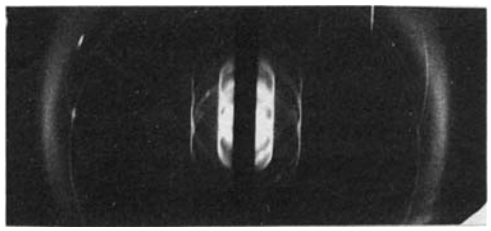

Figure 4. X-ray powder diagram of the S_{B_1} phase of oligosiloxane **B11** obtained with the focusing camera at 114°C.

Above T_m, **B11** and **B5** exhibited in the wide-angle region one sharp reflection (see figure 4), with $d = L$ for **B11**, but $d < L$ for **B5**. Therefore, both structures appear to be monolayer smectics, but of the B type for **B11** and of the F or I type for **B5**. The absence of *hkl* reflections in the X-ray diagrams of the B phase suggests that it is of the hexatic type and not of the crystal type. Due to the relative broadness of the wide-angle diffraction signal, an S_{F_1} phase appeared to occur in **B5**.

Above the transition temperature $T_{S_1-S_2}$ (see table 3), the wide-angle region of **B11** and **B5** exhibited a diffuse band characteristic of a disordered smectic (A or C). Comparison of the smectic layer thickness d with the length L of the repeating unit (see table 4) revealed that **B11** formed an S_{A_1} phase, whereas an S_{C_1} phase with a tilt angle of about 15° was formed in **B5**, as also suggested by optical microscopy observations (see figure 3(*d*)). The differences in the phase structure and sequence of polymers **A5** and **A11**, as opposed to oligomers **B5** and **B11**, reflects the marked influence of their average degree of polymerization on the mesomorphic behaviour.

3.3. *Electron density profiles*

In order to gain further information about the different smectic structures we evaluated the electron density profiles along the director in the orthogonal phases, or along the layer normal in the tilted phases. For that purpose, we put the origin of the z axis, perpendicular to the lamellae, in the middle of the siloxane backbone and

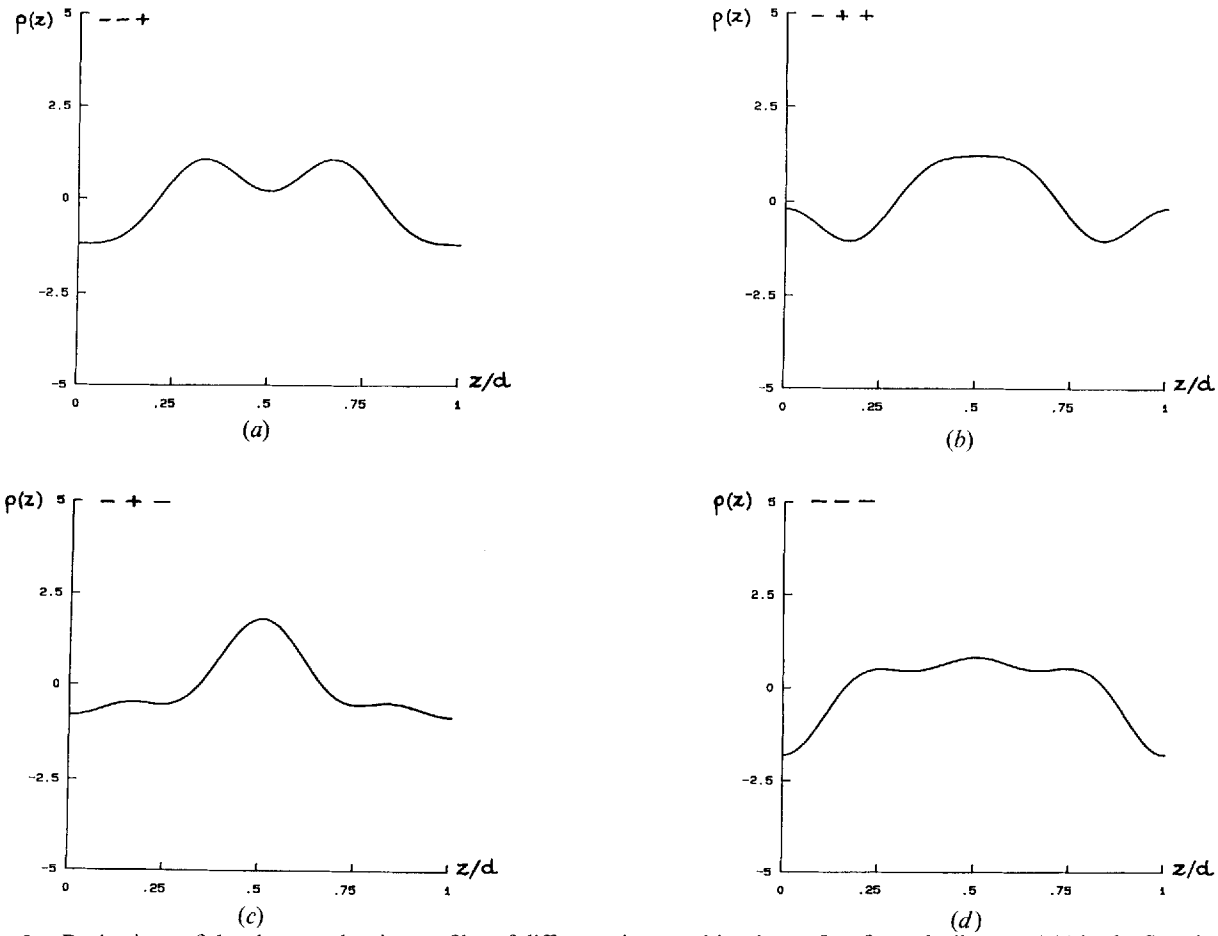

Figure 5. Projections of the electron density profiles of different sign combinations of a_m for polysiloxane **A11** in the S_{A_1} phase: (*a*): ρ_{--+}, (*b*) ρ_{-++}, (*c*) ρ_{+-}, (*d*) ρ_{---}.

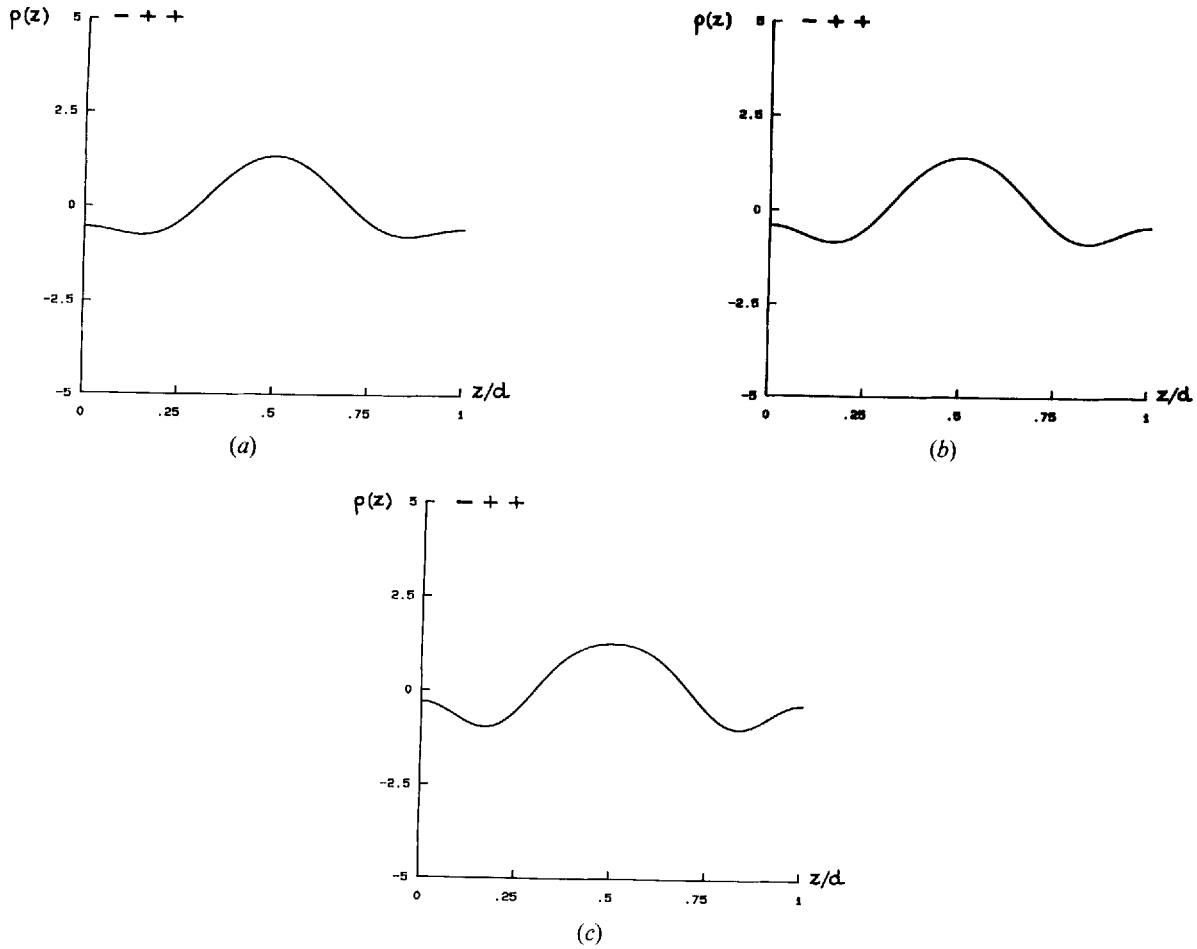

Figure 6. Projections of the electron density profiles of the most physically acceptable sign combination ρ_{-++} for (*a*) the S_{B_1} phase of oligosiloxane **B11**, (*b*) the S_{C_1} phase of oligosiloxane **B5**, and (*c*) the S_{F_1} phase of polysiloxane **A8**.

assumed that as many mesogenic cores are pointing in the $+z$ as in the $-z$ direction. Therefore, $\rho(-z)=\rho(+z)$ and this function of period d could be expressed as a Fourier series containing only the cosine terms [25]

$$\rho(z)=\rho_0+2\Sigma A_m \cos(m2\pi z/d)$$

or

$$\rho(z)=\Sigma a_m \cos(m2\pi z/d)$$

as we only measured the fluctuations of $\rho(z)$ around ρ_0. Nevertheless, the average values, ρ_0, of the projection $\rho(z)$ were easily calculated by dividing the total number of electrons of the polymer repeating unit by the thickness, d, of the smectic layer (see table 1). Experimentally, we measured the intensity I_m of the different orders of reflection, and, as we did not know the sign of a_m, there were 2^m combinations of signs for a_m for any value of m, that is to say 2^m electron density profiles $\rho(z)$ [5]. In order to choose from among them the physically acceptable ones, we calculated the respective electron density of the backbone, the spacer, the mesogenic core, the 2-methylbutoxy tail, and the 2-chloro-3-methylbutanoyloxy tail. Accordingly, the number of electrons of each constituent part was divided by its length, measured using CPK models. We assumed that the spacers adopted an all-*trans*-conformation and also took into account the incompatibility between the polysiloxane backbone and the paraffinic spacer that is known to confine the backbone in a layer of approximately 4 Å thickness. The values of ρ (in e $Å^{-1}$) obtained for the various parts of the repeating unit were 7·8 (backbone), 6·4 (spacer), 10 (biphenylene core), 8 (2-methylbutoxy tail), and 11·8 (2-chloro-3-methylbutanoyloxy tail). From these values, and considering two neighbouring units pointing respectively in the $+z$ and $-z$ direction in the monolayer smectic structures, we could in fact deduce physically acceptable density profiles. In the following, for each type of smectic structure, the electron density profiles corresponding to all the possible combinations of signs will be compared with the physically acceptable ones.

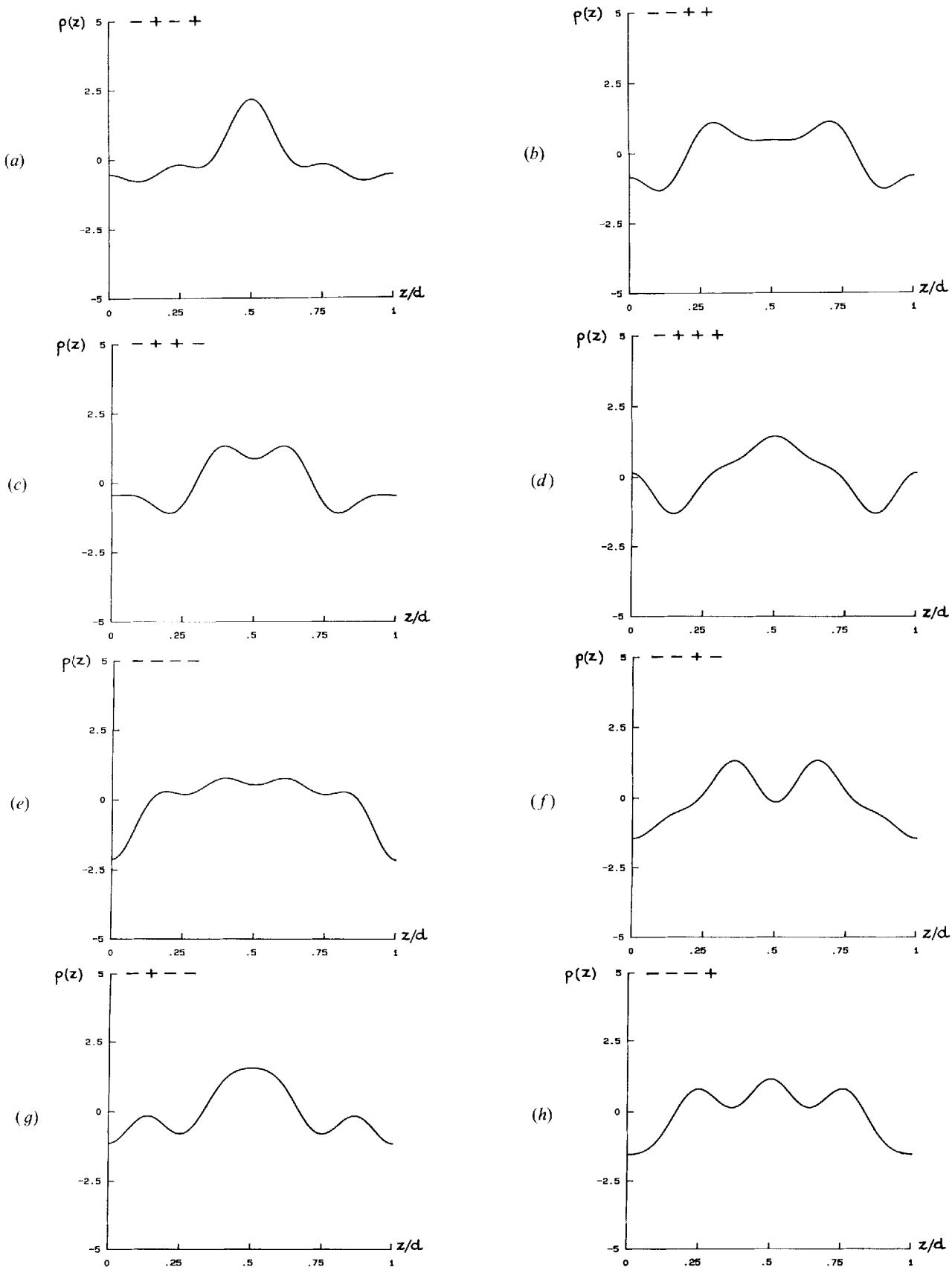

Figure 7. Projections of the electron density profiles of different sign combinations of a_m for polysiloxane **C11** in the S_{A_1} phase: (*a*) ρ_{-+-+}, (*b*) ρ_{--++}, (*c*) ρ_{-++-}, (*d*) ρ_{-+++}, (*e*) ρ_{----}, (*f*) ρ_{--+-}, (*g*) ρ_{-+--}, (*h*) ρ_{---+}.

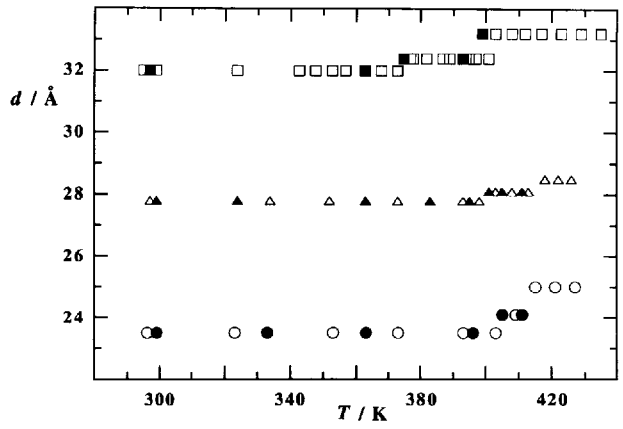

Figure 8. Variation of the thickness, *d*, of the crystalline lamellae or of the smectic layers of polysiloxanes **A11** (□,■), **A8** (△,▲), and **A5** (○,●) on heating (open symbols) and cooling (full symbols).

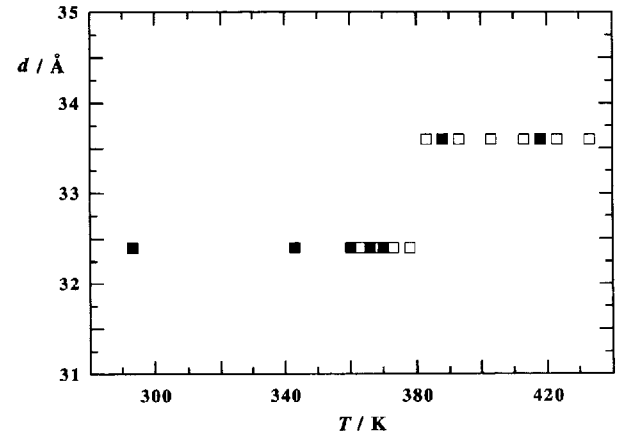

Figure 9. Variations of the thickness, *d*, of the crystalline lamellae or of the smectic layers of polysiloxane **C11** (□,■) on heating (open symbols) and cooling (full symbols).

3.3.1. *Polysiloxanes* **An** *and oligosiloxanes* **Bn**

The X-ray diagrams of the S_{A_1} structure of polymers **A11**, **A8**, and **A5** and oligomer **B11** comprised three sharp low-angle reflections with comparable intensity ratios (see table 1). We will discuss the electron density profile of **A11** as a representative example. The three orders of reflections give rise to eight possible combinations of signs and their corresponding electron density profiles. In figure 5 (*a*)–(*d*) we have represented only four electron density profiles; the other four symmetrical ones were unrealistic, presenting a central minimum at the position of the mesogenic cores, and are not reported. Profile (*a*) did not appear acceptable because it presents a central secondary minimum and two minima for the polysiloxane backbones, while profiles (*c*) and (*d*) are not acceptable in that they show minima for the polysiloxane backbones. The electron density profile (*b*), corresponding to the combination of signs $-++$, that exhibits a maximum for the mesogenic cores in the middle of the layers and secondary maxima at the siloxane backbones on the borders of the layers seemed to be the most reasonable solution. The same arguments led us to choose the electron density profile ρ_{-++} for **A5**, **A8**, and **B11** too.

The X-ray diagrams of the S_{C_1} and S_{F_1} structures of **A11**, **A8**, **A5**, and **B5**, and of the S_{B_1} structure of **B11**, displayed, in the low-angle region, three sharp reflections with intensity ratios comparable with each other and with those of the respective S_{A_1} phase. Consistent with the above discussion, the electron density profile corresponding to the combinations of signs $-++$ was selected as the most physically acceptable one. Only these electron density profiles are given in figure 6.

Therefore, for all the smectic structures of all these polymers and oligomers the appropriate combination of signs was the same, independent of the length of the methylene spacer. Furthermore, the electron density profile corresponding to that combination of signs was in agreement with the monolayer character of the smectic phases and with a microsegregation between the siloxane backbones and the side chains.

3.3.2. *Polysiloxane* **C11**

The introduction of a chlorine atom in the tail close to the mesogenic core of **C11** was expected to result in a rather different electron density profile. The X-ray diffraction patterns of the S_{A_1} phase consisted, in the low-angle region, of four orders of reflections (see table 1). Among the sixteen possible electron density profiles, the eight presenting minima at the positions of the mesogenic cores and the chlorine atoms were evidently discarded and are not represented in figure 7 (*a*)–(*h*). Electron density profiles (*e*)–(*h*) exhibited minima at the positions of the polysiloxane backbones. In profiles (*a*) and (*d*), a maximum was seen at the centre of the lamellae, where the mesogenic cores are situated, but not at the positions of the chlorine atoms that, in contrast, dominate the electron density profile of the repeating unit. Profiles (*b*) and (*c*) were both characterized by two secondary maxima at the positions of the polysiloxane backbone and two main maxima, but in (*c*) the major maxima corresponded to the mesogenic core, whereas the chlorine atoms corresponded to minima. Therefore, electron density profile ρ_{--++} (see figure 7 (*b*)) seemed the most realistic one that comprised a central plateau corresponding to the mesogenic cores flanked by two main maxima at the positions of the chlorine atoms, two

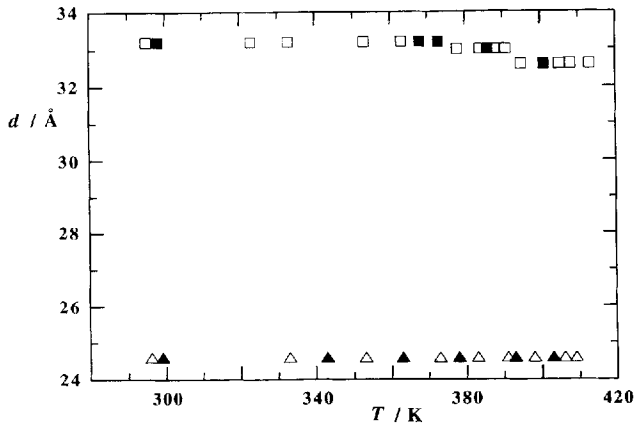

Figure 10. Variation of the thickness, d, of the crystalline lamellae or of the smectic layers of oligosiloxanes **B11** (□,■) and **B5** (△,▲) on heating (open symbols) and cooling (full symbols).

minima at the positions of the methylene spacers, and two secondary maxima at the positions of the polysiloxane backbones. This profile is in agreement with the hierarchy of the electron densities of the different parts of the repeating units of the polymer.

3.4. *Influence of temperature*

Figures 8, 9, and 10 show the variation with temperature of the thickness d of the crystalline lamellae or of the smectic layers for polysiloxanes **An** and **C11** and oligosiloxanes **Bn**, respectively. Within the whole temperature range of existence of any one phase (C, S_{A_1}, S_{B_1}, S_{C_1}, or S_{F_1}), d was independent of temperature and remained constant. No changes in the smectic layer periodicity were detected at the S_{F_1}–S_{C_1} transition (see, for example, figure 9). Therefore, the tilt angle remained essentially unaffected. More significant variations of d could be detected at the S_{A_1}–S_{C_1} transition (see, for example, figure 8), consistent with a change from an orthogonal mesophase to a tilted one. The values of the structural parameters found on heating were reversibly obtained on cooling, except for **C11**, for which the ordered smectic structure remained frozen in at room temperature. For both classes of materials, d increased with the number n of methylene groups of the spacer.

4. Concluding remarks

The structure of the phases formed by liquid crystalline polysiloxanes and oligosiloxanes was elucidated by X-ray diffraction analysis of powder samples and of oriented samples, whenever it was possible to draw fibres (**A11**, **A8**, and **A5**). We found three types of semicrystalline phases (possibly three-dimensionally ordered smectics) and four types of monolayer smectics, that is S_{A_1}, S_{B_1}, S_{C_1}, and S_{F_1} (or S_{I_1}) phases. In addition, we drew the projection of the electron density profiles along the layer normal and deduced the physically acceptable electron density profile from among the numerous possibilities for each smectic phase. We found that, for any type of phase, the physically acceptable combination of signs was the same for all the oligomers and polymers with a 2-methylbutoxy tail that formed this type of smectic phase. For a given polymer (**A11**) or oligomer (**B11**), the most realistic combination of signs was the same for the different smectic phases. Furthermore, the electron density profiles were in agreement with monolayer smectic phases presenting a microphase separation between the siloxane backbones and the side chains, constraining the backbones in a thin layer. In recent publications [17] and references therein, and [26], the investigation of electron density profiles was used to describe the mesophase structure of several side chain liquid crystalline polymers. In particular, for the set of polysiloxanes analysed with phenyl benzoate side chains, the sign combinations chosen for the physically acceptable electron density profile were the same for all the polymers in both the A_1 and B_1 phases [17]. Furthermore, a microphase separation of the polymer backbone and the mesogenic side chains was evidenced, by analogy with the present results. Whether these may be general features for side chain polysiloxanes has to be ascertained by means of more systematic investigations.

Our X-ray diffraction studies have also shown that independent of the spacer length and the tail nature, the polysiloxanes underwent the same sequence of phases C–S_{F_1}–S_{C_1}–S_{A_1}–I, whereas the oligosiloxanes gave the sequence C–S_{B_1}–S_{A_1}–I (**B11**) or C–S_{F_1}–S_{C_1}–I (**B5**). The existence of three mesophases in the polymers and only two mesophases in the oligomers probably results from the fact that the ordering power of the backbone decreases with its average degree of polymerization. Furthermore, in the polymers, the length of the spacer had no influence on the nature and the succession of the phases. In contrast, when the length of the spacer of the oligomers decreased from eleven to five methylene groups, the orthogonal structures (S_{B_1} and S_{A_1}) turned into tilted structures (S_{F_1} and S_{C_1}). The structure originated by the materials might result in fact from the interplay of the antagonist influences of the backbone and the spacer. When the degree of polymerization decreased, the influence of the main chain decreased in parallel and the length of the spacer became prominent in determining the nature of the phases. Longer spacers tended to favour the onset of orthogonal phases, while shorter spacers permitted the formation of tilted phases.

We recently found [12] that polyacrylates comprising the same 4′-((*S*)-2-methylbutoxy)biphenylene side chains connected to the polymer backbone by flexible spacers of

varying number, n, of methylene groups gave rise to bilayer S_{A_2} phases ($n=5$ or 6), partly interdigitated S_{A_d} ($n=7$), and monolayer S_{A_1} structures ($n=8$ to 11). In contrast, the present polysiloxanes invariably formed monolayer structures when n varied from 5 to 11. This behaviour can be explained by the greater stiffness of the polyacrylate backbone that allows the existence of bilayer structures in which the intralayer interactions between mesogenic groups are lower. In contrast, the more flexible polysiloxane chain appears to facilitate the adoption of monolayer structures in which the interactions among neighbouring side chain mesogens may be maximized.

This work was performed with financial support from Progetti Bilaterali of the Italian CNR and the French CNRS, and from the Ministero dell'Università e della Ricerca Scientifica of Italy.

References

[1] ESCHER, C., and WINGEN, R., 1992, *Adv. Mater.*, **4,** 189.
[2] MEYER, R. B., LIEBERT, L., STRZELECKI, L., and KELLER, P., 1975, *J. Phys. Lett., Paris*, **36,** L69.
[3] 1993, *4th International Conference on Ferroelectric Liquid Crystals*, Tokyo, Japan, *Abstracts*
[4] CHIELLINI, E., GALLI, G., CIONI, F., and DOSSI, E., 1993, *Makromolek. Chem., Macromolek. Symp.*, **69,** 51.
[5] DAVIDSON, P., and LEVELUT, A. M., 1992, *Liq. Crystals*, **11,** 469.
[6] DAVIDSON, P., KÜHNPAST, K., SPRINGER, J., and SCHEROWSKY, G., 1993, *Liq. Crystals*, **14,** 901.
[7] KÜHNPAST, K., SPRINGER, J., DAVIDSON, P., and SCHEROWSKY, G., 1992, *Makromolek. Chem.*, **193,** 3097.
[8] SCHEROWSKY, G., KÜHNPAST, K., and SPRINGER, J., 1991, *Makromolek. Chem. rap. Commun.*, **12,** 381.
[9] BÖMELBURG, J., HEPPKE, G., and HOLLIDT, J., 1991, *Makromolek. Chem. rap. Commun.*, **12,** 483.
[10] SKARP, K., ANDERSSON, G., GOUDA, F., LAGERWALL, S. T., POTHS, H., and ZENTEL, R., 1992, *Polym. Adv. Technol.*, **3,** 241.
[11] CHIELLINI, E., GALLI, G., DOSSI, E., CIONI, F., and GALLOT, B., 1993, *Macromolecules*, **26,** 849.
[12] CHIELLINI, E., GALLI, G., CIONI, F., DOSSI, E., and GALLOT, B., 1993, *J. mater. Chem.*, **3,** 1065.
[13] CHIELLINI, E., GALLI, G., ANGELONI, A. S., and LAUS, M., 1993, *Organic Materials for Non-linear Optics*, Vol. III, edited by G. J. Ashwell and D. Bloor (Royal Society of Chemistry), p. 169.
[14] KOMITOV, L., LAGERWALL, S. T., STEBLER, B., CHIELLINI, E., GALLI, G., and STRIGAZZI, A., 1993, *Modern Topics in Liquid Crystals*, edited by A. Buka (World Scientific), p. 301.
[15] CHIELLINI, E., GALLI, G., KOMITOV, L., LAGERWALL, S. T., STEBLER, B., and STRIGAZZI, A., 1994, Eur. Pat. Appl.
[16] CHIELLINI, E., GALLI, G., and CIONI, F., 1991, *Ferroelectrics*, **114,** 223.
[17] DAVIDSON, P., LEVELUT, A. M., ACHARD, M. F., and HARDOUIN, F., 1989, *Liq. Crystals*, **4,** 561, and references therein.
[18] GRAY, G. W., and GOODBY, J. W., 1984, *Smectic Liquid Crystals* (Leonard Hill).
[19] DOUCET, J., 1979, *The Molecular Physics of Liquid Crystals*, edited by G. R. Luckhurst and G. W. Gray (Academic Press), p. 317.
[20] BENATTAR, J. J., MOUSSA, F., and LAMBERT, M., 1983, *J. Chim phys.*, **80,** 99. GANE, P. A. C., LEADBETTER, A. J., BENATTAR, J. J., MOUSSA, F., and LAMBERT, M., 1981, *Phys. Rev.* A, **24,** 2694.
[21] TABRIZIAN, M., BUNEL, C., VAIRON, J.-P., FRIEDRICH, C., and NOEL, C., 1993, *Makromolek. Chem.*, **194,** 891.
[22] BAHR, C., and HEPPKE, G., 1986, *Molec. Crystals liq. Crystals, Lett.*, **4,** 31.
[23] KOMITOV, L., LAGERWALL, S. T., GALLI, G., and CHIELLINI, E. (in preparation).
[24] GANE, P. A. C., LEADBETTER, A. J., and WRIGHTON, P. G., 1981, *Molec. Crystals liq. Crystals*, **66,** 247.
[25] GUDKOV, V. A., 1984, *Soviet Phys. Crystallogr.*, **29,** 316.
[26] FRANCESCANGELI, O., YANG, B., CHIELLINI, E., GALLI, G., ANGELONI, A. S., and LAUS, M., 1993, *Liq. Crystals*, **14,** 981.